JOURNAL OF AIRCRAFT
Vol. 43, No. 5, September–October 2006

Sensitivities and Approximations for Aeroservoelastic Shape Optimization with Gust Response Constraints

Marat Mor* and Eli Livne†
University of Washington, Seattle, Washington 98195-2400

DOI: 10.2514/1.17467

Analytic sensitivities with respect to configuration shape design variables are derived for state-space models of aeroservoelastic systems excited by gust inputs. Minimum-state rational function approximations are used to transform aerodynamic load expressions from the frequency domain to the time domain, and sensitivities of such approximations are extended from terms associated with structural motions to terms associated with the downwash due to gusts. Sensitivity-based approximations of the resulting gust response behavior, including Taylor-series based direct approximations of the rms of the response, or Lyapunov equation solutions using Taylor-series based approximate system matrices are compared. The paper contributes to the development of design-oriented analysis techniques for multidisciplinary design optimization of flight vehicles.

Nomenclature

$[A_e]$, $[B_e]$, $[C_e]$	=	state-space model matrices of gust delay rational transfer function [defined in Eqs. (28) and (29)]
$[A_G]$, $[B_G]$, $[C_G]$	=	state-space model matrices of gust filter [defined in Eq. (45)]
$[A_0]$, $[A_1]$, $[A_2]$, ...	=	rational approximation matrices
a	=	low pass filter parameter [Eq. (43)]
$\{B\}$	=	state-space white noise input vector
b	=	reference semichord length of wing
$[C]$	=	damping matrix
$[D]$, $[E]$	=	rational approximation matrices of lag terms
DV	=	design variable
E	=	Young modulus
G	=	shear modulus
H_G	=	gust-filter transfer function [defined in Eq. (43)]
$[I]$	=	identity matrix
j	=	pure imaginary number, $j = -\sqrt{1}$
$[K]$	=	stiffness matrix
k	=	reduced frequency
L	=	distance to the reference point of certain gust zone
$[L]$	=	state-space model aeroelastic matrix
l_G	=	scale of turbulence
$[M]$	=	mass matrix
m	=	number of gust vectors approximated together
n	=	number of states
n_e	=	order of the gust delay rational approximation
n_G	=	number of gust zones
n_{lag}	=	number of lag terms
$[Q]$	=	aerodynamic generalized force coefficient matrix
q_D	=	dynamic pressure
$[R]$	=	diagonal matrix of lag roots
s	=	Laplace variable
T	=	time takes gust to reach a reference point of certain gust zone
t	=	time
V	=	speed of flight
w	=	white noise
$\{w_G\}$	=	vector of vertical gust velocity inputs
$[X]$	=	covariance matrix of the state-space vector $\{x\}$
$\{x\}$	=	state vector [Eq. (46)]
$\{x_e\}$	=	state vector related to gust delay [Eq. (27)]
$\{x_G\}$	=	state vector related to gust filter [Eq. (44)]
$\{x_{G_{\text{lag}}}\}$	=	vector of aerodynamic states related to gust [Eqs. (15) and (16)]
$\{x_{\text{lag}}\}$	=	vector of aerodynamic states [Eq. (14)]
Y_t, Y_w	=	half-span length of tail and wing, respectively
α	=	induced angle of attack
γ	=	roots of lag terms
Δ	=	sweep angle of wing
ζ	=	damping ratio
λ	=	poles
$\{\xi\}$	=	vector of generalized structural dynamic motions
ρ	=	density
σ	=	covariance
σ_{w_G}	=	gust rms
τ_G	=	defined in Eq. (42)
$[\Phi]$	=	matrix of eigenvectors
ω	=	frequency of oscillation

Subscripts and Superscripts

F	=	flutter
G	=	gust
max	=	maximum value
REF	=	reference design point
ref	=	reference point related to gust (the point where gust is measured)

Presented as Paper 2077 at the 46th Structures, Structural Dynamics, and Materials Conference, Austin, Texas, 18–21 April 2005; received 1 May 2005; revision received 9 November 2005; accepted for publication 26 November 2005. Copyright © 2006 by Marat Mor and Eli Livne. Published by the American Institute of Aeronautics and Astronautics, Inc., with permission. Copies of this paper may be made for personal or internal use, on condition that the copier pay the $10.00 per-copy fee to the Copyright Clearance Center, Inc., 222 Rosewood Drive, Danvers, MA 01923; include the code $10.00 in correspondence with the CCC.

*Post Doctoral Research Fellow, Department of Aeronautics and Astronautics; mor@aa.washington.edu. Member AIAA.

†Professor, Department of Aeronautics and Astronautics; eli@aa.washington.edu. Associate Fellow AIAA.

t	=	tail
tr, tt	=	tail's root and tip respectively
w	=	wing
wr, wt	=	wing's root and tip, respectively
z	=	z direction

Functions and Operators

~	=	"combine" operator [see Eqs. (30) and (31)]
$\bar{I}$	=	defines the division of gust zones approximated together
I	=	relates to the $\bar{I}$ division of gust zones [defined in Eq. (35)]. Used to combine filters of gust delay into one division
II	=	defines the division of gust zones approximated separately [defined in Eq. (39)]

I. Introduction

CONFIGURATION shape variations, during the design optimization of flight vehicles, make it necessary to remesh for and recalculate unsteady aerodynamic forces with every shape change. Even in the case of linearized aerodynamics, used successfully for aeroservoelastic analysis of flight vehicles over the last 30 years, the computational effort required for the repetitive generation of unsteady aerodynamic influence coefficient matrices and generalized loads is significant. The problem becomes more demanding when frequency-domain unsteady aerodynamic force coefficients are transformed into the time domain using rational function approximations. When the minimum-state (MIST) rational function approximation is used [1], leading to reduced order coupled aeroservoelastic time-domain mathematical models, its generation process is iterative, lengthy, suffers from a nonuniqueness problem, and in practical applications it has to be stopped before full convergence is reached. These issues make the calculation of sensitivities of time domain unsteady aerodynamic terms with respect to shape design variables difficult. Such sensitivities are important, because they can be used to construct approximate expressions for the unsteady aerodynamic force terms in terms of shape design variables, and thus, help to accelerate the repetitive generation of aeroservoelastic models considerably [2]. In a previous paper [3] a method for calculating shape sensitivities and approximations of time-domain unsteady aerodynamic forces and aeroservoelastic models was presented.

Exploratory studies in [3] focused on the stability (flutter) problem. The goal of the present paper is to extend the techniques described in [3] to cases where gust aerodynamic columns are present in the unsteady aerodynamic matrices, and to study shape sensitivity calculation and approximation techniques in the case of the gust response problem.

This extension is challenging, because unsteady aerodynamic gust force elements can have complex dependency on reduced frequency for simple harmonic motions [4], and because this complex behavior is difficult to capture by time-domain rational function approximations such as the Roger and minimum-state approximations. The problem is especially severe in the case of configurations with highly swept wing and wing/horizontal tail combinations. The paper opens with a complete derivation of state-space equations for general flight vehicle configurations excited by gust inputs, where gust inputs over separate zones are transformed from the frequency domain to the time domain separately, and then linked to a single gust input for the configuration. Analytic sensitivities of all state-space matrices are then derived, followed by analytic sensitivities of the state covariance matrix and rms values of individual responses. Accuracy of the new sensitivity expressions and alternative behavior approximations based on those sensitivities is finally evaluated.

II. Time-Domain Aeroelastic Equations for Gust Response

A. Aeroelastic System Excited by Gust Inputs at Different Gust Zones

The linear aeroelastic problem (corresponding to structural degrees of freedom) including gust excitation can be formulated in the Laplace domain as follows:

$$(s^2[M] + s[C] + [K] - q_D[Q(s)])\{\xi(s)\} = q_D[Q_G(s)]\left\{\frac{w_G(s)}{V}\right\} \tag{1}$$

where $[Q(s)]_{n\times n}$ is the Laplace-transformed generalized aerodynamic force coefficient matrix, $[M]_{n\times n}$, $[C]_{n\times n}$, $[K]_{n\times n}$ are structural inertial, viscous damping, and stiffness matrices, respectively, q_D is dynamic pressure, and n is the number of states. The vector of generalized structural dynamic motions is $\{\xi(s)\}$.

In Eq. (1) the gust excitation $[Q_G(s)]$ is a Laplace-transformed aerodynamic force coefficient matrix. The gust terms as functions of reduced frequency usually have a complex frequency-dependent spiral nature [4,5]. For linear-time-invariant (LTI) state-space aeroservoelastic formulations, such frequency-dependent functions must be approximated by rational transfer functions in the Laplace variable. It is unlikely to get an adequate approximation of a general gust column in a form of ratios of polynomials in s. However, the source of spiral behavior of gust force terms as functions of reduced frequency had been identified as determined by the reference point used for the sinusoidal waves representing the gust field [4].

To overcome this problem (and following [4,5], the aerodynamic model for gust force generation is divided into n_G zones as will be explained later, with a separate gust speed input for each zone. Then the dimension of the Laplace-transformed aerodynamic force coefficient matrix $[Q_G(s)]$ is $n \times n_G$. In addition, $\{w_G(s)\}_{n_G}$ is the vector of vertical gust velocity inputs to the different zones and V is the free stream velocity.

Using the MIST method the $[Q]$ matrix is approximated in the form of a rational function:

$$[Q(jk)]_{n\times n} \approx [A_0]_{n\times n} + jk[A_1]_{n\times n} + (jk)^2[A_2]_{n\times n} + jk[D]_{n\times n_{\text{lag}}}(jk[I] - [R])^{-1}_{n_{\text{lag}}\times n_{\text{lag}}}[E]_{n_{\text{lag}}\times n} \tag{2}$$

Here n_{lag} is the number of aerodynamic lag terms and k is a reduced frequency defined as

$$k = \frac{\omega b}{V} \Rightarrow jk = \frac{b}{V}s \tag{3}$$

where b is a reference semichord length and ω is a frequency of oscillation. $[R]$, a diagonal matrix corresponding to the generalized aerodynamic force, contains the aerodynamic (positive) lag roots, which are selected by the user

$$[R]_{n_{\text{lag}}\times n_{\text{lag}}} = -\begin{bmatrix} \gamma_1 & 0 & \dots & 0 \\ 0 & \gamma_2 & \dots & 0 \\ \dots & \dots & \dots & \dots \\ 0 & 0 & \dots & \gamma_{n_{\text{lag}}} \end{bmatrix} \tag{4}$$

A MIST approximation can be generated for the combined $[Q|Q_G]$ matrices as follows:

$$\{[Q(jk)]_{n\times n} \quad [Q_G(jk)]_{n\times n_G}\} \approx \{[A_0]_{n\times n} \quad [A_{G_0}]_{n\times n_G}\} + jk\{[A_1]_{n\times n} \quad [A_{G_1}]_{n\times n_G}\} + (jk)^2\{[A_2]_{n\times n} \quad [0]_{n\times n_G}\} + jk[D]_{n\times n_{\text{lag}}}(jk[I] - [R])^{-1}_{n_{\text{lag}}\times n_{\text{lag}}}\{[E]_{n_{\text{lag}}\times n} \quad [E_G]_{n_{\text{lag}}\times n_G}\} \tag{5}$$

where n_G is the number of gust input columns. However, because in the MIST approximation the $[D]$, $[E]$ matrices are determined simultaneously and affect one another, the presence of $[E_G]$ columns can affect the $[D]$ matrix, and, thus, the quality of approximation of the $[Q]$ matrix.

In the formulation proposed here the MIST approximation of gust columns will be done separately from the generalized aerodynamic force coefficient matrix $[Q]$ corresponding to structural modes of motion. Despite the fact that this might increase the number of states in the state-space model, the approximation for $[Q]$ (generalized aerodynamic forces due to motion in structural modes) is now independent of the gust generalized forces, therefore allowing more flexibility for capturing the behavior of the matrix $[Q]$ more accurately, separately from the influence of the high-frequency spiral behavior of the gust aerodynamic matrix.

Dividing the gust aerodynamic force into zones increases the number of aerodynamic states. But one can reduce this number if it is observed that gust force vector terms of certain zones can be grouped together and approximated together with good accuracy. The gust force vectors are sorted into two divisions. The first division includes m gust vectors (from 1 to m) whose spiral behaviors are similar and who can be combined into one zone that will yield satisfactory MIST approximation for that combined zone. The rest of the gust vectors (from $m+1$ up to n_G), when the frequency-dependent behavior of gust vectors in different zones are highly dissimilar, are approximated separately, and this gives more flexibility to the user and more precision to the final approximation (see Appendix A).

The gust force contribution can then be rewritten in the following manner:

$$q_D[Q_G(s)]_{n\times n_G}\left\{\frac{w_G(s)}{V}\right\}_{n_G} = q_D\sum_{i=1}^{n_G}\{Q_G^i(s)\}_n\frac{w_G^i(s)}{V}$$
$$= q_D[Q_G^{\bar{I}}(s)]_{n\times m}\left\{\frac{w_G^{1\sim m}(s)}{V}\right\}_m + q_D\sum_{i=m+1}^{n_G}\{Q_G^i(s)\}_n\frac{w_G^i(s)}{V} \quad (6)$$

where

$$\{w_G(s)\}_{n_G} = \begin{Bmatrix}\{w_G^{1\sim m}(s)\}_m\\ w_G^{m+1}(s)\\ \dots\\ \dots\\ w_G^{n_G}(s)\end{Bmatrix} \quad (7)$$

$\{w_G^{1\sim m}(s)\}$ is the gust vector related to the first division gust forces, whose aerodynamic matrix $[Q_G^{\bar{I}}(s)]$ is column partitioned

$$[Q_G^{\bar{I}}(s)]_{n\times m} = \begin{bmatrix}\{Q_G^1\}_n & \{Q_G^2\}_n & \dots & \{Q_G^m\}_n\end{bmatrix} \quad (8)$$

and approximated using the MIST double least-squares iterative method

$$[Q_G^{\bar{I}}]_{n\times m} \approx [A_{G_0}^{\bar{I}}]_{n\times m} + jk[A_{G_1}^{\bar{I}}]_{n\times m} + jk[D_G^{\bar{I}}]_{n\times n_{G_{\text{lag}}}^{\bar{I}}}$$
$$\times\left(jk[I] - \frac{V}{b}[R_G^{\bar{I}}]\right)^{-1}_{n_{G_{\text{lag}}}^{\bar{I}}\times n_{G_{\text{lag}}}^{\bar{I}}}[E_G^{\bar{I}}]_{n_{G_{\text{lag}}}^{\bar{I}}\times m} \quad (9)$$

The rest of the gust columns are approximated each separately, using MIST/Roger [3] methods (in this case the MIST problem becomes identical to the Roger problem, and therefore, the approximation is solved without iterations through a single least-squares step), adding additional $n_{G_{\text{lag}}}^i$ defined by user for each $i = m+1,\dots n_G$

$$\{Q_G^i\}_n \approx \{A_{G_0}^i\}_n + jk\{A_{G_1}^i\}_n + jk[D_G^i]_{n\times n_{G_{\text{lag}}}^i}(jk[I] - [R_G^i])^{-1}_{n_{G_{\text{lag}}}^i\times n_{G_{\text{lag}}}^i}$$
$$\times\{E_G^i\}_{n_{G_{\text{lag}}}^i}, \qquad i = m+1,\dots n_G \quad (10)$$

In Eqs. (9) and (10) $[R_G^{\bar{I}}]$ and $[R_G^i]$,

$$i = m+1,\dots,n_G$$

[similar to the lag matrix $[R]$, Eq. (4)] are the diagonal lag-terms matrices corresponding to the aerodynamic forces due to gust excitation with the user selected positive lag roots

$$[R_G^{\bar{I}}]_{n_{G_{\text{lag}}}^{\bar{I}}\times n_{G_{\text{lag}}}^{\bar{I}}} = -\begin{bmatrix}\gamma_{G_1}^{\bar{I}} & 0 & \dots & 0\\ 0 & \gamma_{G_2}^{\bar{I}} & \dots & 0\\ \dots & \dots & \dots & \dots\\ 0 & 0 & \dots & \gamma_{G_{n_{G_{\text{lag}}}^{\bar{I}}}}^{\bar{I}}\end{bmatrix} \quad (11)$$

$$[R_G^i]_{n_{G_{\text{lag}}}^i\times n_{G_{\text{lag}}}^i} = -\begin{bmatrix}\gamma_{G_1}^i & 0 & \dots & 0\\ 0 & \gamma_{G_2}^i & \dots & 0\\ \dots & \dots & \dots & \dots\\ 0 & 0 & \dots & \gamma_{G_{n_{G_{\text{lag}}}^i}}^i\end{bmatrix}$$
$$i = m+1,\dots n_G \quad (12)$$

where $n_{G_{\text{lag}}}^{\bar{I}}$ and $n_{G_{\text{lag}}}^i$,

$$i = m+1,\dots n_G$$

are the numbers of gust aerodynamic lag terms related to the first and the second divisions of the gust forces, respectively.

Substituting Eqs. (2–4) together with Eqs. (9–12) into Eq. (1) one obtains a new approximate system of equations in the Laplace domain:

$$\left\{s^2[\bar{M}] + s[\bar{C}] + [\bar{K}] - q_D[D]s\left([I]s - \frac{V}{b}[R]\right)^{-1}[E]\right\}\{\xi(s)\}$$
$$= q_D\left\{[A_{G_0}^{\bar{I}}] + s\frac{b}{V}[A_{G_1}^{\bar{I}}] + [D_G^{\bar{I}}]s\left([I]s - \frac{V}{b}[R_G^{\bar{I}}]\right)^{-1}[E_G^{\bar{I}}]\right\}$$
$$\times\left\{\frac{w_G^{1\sim m}(s)}{V}\right\} + q_D\sum_{i=m+1}^{n_G}\left[\left\{A_{G_0}^i\right\} + s\frac{b}{V}\left\{A_{G_1}^i\right\}\right.$$
$$\left. + [D_G^i]s\left([I]s - \frac{V}{b}[R_G^i]\right)^{-1}\{E_G^i\}\right]\frac{w_G^i(s)}{V} \quad (13)$$

Introducing vectors of aerodynamic states (Laplace-transformed) as follows:

$$\{x_{\text{lag}}(s)\}_{n_{\text{lag}}} = s\left([I]s - \frac{V}{b}[R]\right)^{-1}_{n_{\text{lag}}\times n_{\text{lag}}}[E]_{n_{\text{lag}}\times n}\{\xi(s)\}_n \quad (14)$$

and similar, the lag states related to gust

$$\left\{x_{G_{\text{lag}}}^{1\sim m}(s)\right\}_{n_{G_{\text{lag}}}^{\bar{I}}} = s\left([I]s - \frac{V}{b}[R_G^{\bar{I}}]\right)^{-1}_{n_{G_{\text{lag}}}^{\bar{I}}\times n_{G_{\text{lag}}}^{\bar{I}}}[E_G^{\bar{I}}]_{n_{G_{\text{lag}}}^{\bar{I}}\times m}\left\{\frac{w_G^{1\sim m}(s)}{V}\right\}_m \quad (15)$$

$$\left\{x_{G_{\text{lag}}}^i(s)\right\}_{n_{G_{\text{lag}}}^i} = s\left([I]s - \frac{V}{b}[R_G^i]\right)^{-1}_{n_{G_{\text{lag}}}^i\times n_{G_{\text{lag}}}^i}\{E_G^i\}_{n_{G_{\text{lag}}}^i}\frac{w_G^i(s)}{V}$$
$$i = m+1,\dots n_G \quad (16)$$

Equation (13) is finally transformed into

$$(s^2[\bar{M}] + s[\bar{C}] + [\bar{K}])\{\xi(s)\} - q_D[D]\{x_{\text{lag}}(s)\}$$
$$= q_D\left([A_{G_0}] + s\frac{b}{V}[A_{G_1}]\right)\left\{\frac{w_G(s)}{V}\right\} + q_D[D_G^{\bar{I}}]\left\{x_{G_{\text{lag}}}^{1\sim m}(s)\right\}$$
$$+ q_D\sum_{i=m+1}^{n_G}[D_G^i]\left\{x_{G_{\text{lag}}}^i(s)\right\} \quad (17)$$

Here

$$[\bar{M}] = [M] - q_D\left(\frac{b}{V}\right)^2[A_2], \qquad [\bar{C}] = [C] - q_D\frac{b}{V}[A_1]$$
$$[\bar{K}] = [K] - q_D[A_0] \quad (18)$$

and the matrices $[A_{G_0}]$, $[A_{G_1}]$ are column partitioned as follows:

$$[A_{G_0}]_{n\times n_G} = \left[\, [A^{\bar{I}}_{G_0}]_{n\times m} \quad \{A^{m+1}_{G_0}\}_n \quad \dots \quad \{A^{n_G}_{G_0}\}_n \,\right]$$
$$[A_{G_1}]_{n\times n_G} = \left[\, [A^{\bar{I}}_{G_1}]_{n\times m} \quad \{A^{m+1}_{G_1}\}_n \quad \dots \quad \{A^{n_G}_{G_1}\}_n \,\right] \tag{19}$$

B. Gust Input Linking

The formulation for aerodynamic gust columns generation is similar to the one in [6]. The discrete gust profile of the vertical velocity $w^{\text{ref}}_G(t)$ is defined at a reference point $x = x_{\text{ref}}$ and it is moving towards the vehicle with the axial velocity V (see Fig. 1). As was discussed previously, the gust input is divided into n_G zones (i.e., sets of aerodynamic panels), each zone with its own reference point. The gust on the ith zone $w^i_G(t)$ is delayed with respect to the gust measured at the reference point $w^{\text{ref}}_G(t)$

$$w^i_G(t) = w^{\text{ref}}_G(t - T_i), \qquad i = 1, \dots n_G \tag{20}$$

where T_i is the time that it takes for the gust to reach the reference point of the ith zone x_i after passing the reference point x_{ref}

$$T_i = \frac{x_i - x_{\text{ref}}}{V} = \frac{L_i}{V} \tag{21}$$

Laplace transformation of Eq. (20) leads to

$$w^i_G(s) = w^{\text{ref}}_G(s) e^{-T_i s} \tag{22}$$

To create a LTI state-space model of the gust-excited aeroelastic system the exponential function in Eq. (22) has to be approximated by a rational function in s. This means added states, and the number depends on the order of the polynomial approximation of $e^{-T_i s}$.

Comparing the coefficients of this exponent expanded into Taylor series to the coefficients of the polynomial ratio (see Appendix B), one can find approximations of different orders. Figure 2 shows the behavior of the third order

$$e^{-T_i s} \approx 3\frac{(T_i s)^2 - 8T_i s + 20}{(T_i s)^3 + 9(T_i s)^2 + 36T_i s + 60} \tag{23a}$$

and the fourth order

$$e^{-T_i s} \approx -4\frac{(T_i s)^3 - 15(T_i s)^2 + 90T_i s - 210}{(T_i s)^4 + 16(T_i s)^3 + 120(T_i s)^2 + 480T_i s + 840} \tag{23b}$$

approximations. A commonly used approximation

$$e^{-T_i s} \approx \left(1 + \frac{T_i s}{n_e}\right)^{-n_e} \tag{24}$$

of the fourth order is also presented. One can see that the accuracy of this approximation is low compared with the rest. Substituting $s = j\omega$ together with Eqs. (3) and (21) the following relation (connecting ωT in Fig. 2 to the reduced frequency k) is obtained:

$$\omega T_i = \frac{L_i}{b} k \tag{25}$$

Based on Fig. 2, one can find that in order to accurately approximate the gust aerodynamic force coefficient matrix in the problems where the gust zones are used, the maximum reduced frequency has to satisfy

$$k_{\max} < 3\frac{b}{L_{\max}} \tag{26a}$$

for the third order, and

$$k_{\max} < 5\frac{b}{L_{\max}} \tag{26b}$$

for the fourth order rational approximations of $e^{-T_i s}$. [Typically, the third order approximation in Eq. (23a) is good enough for the gust problems.]

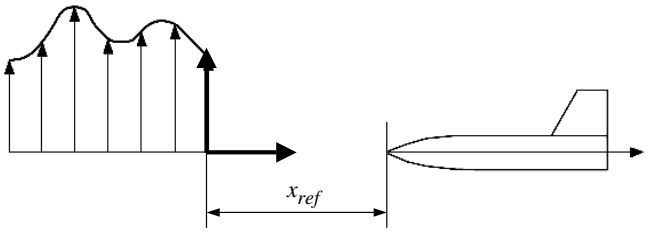

Fig. 1 Traveling discrete gust profile excitation (from [5]).

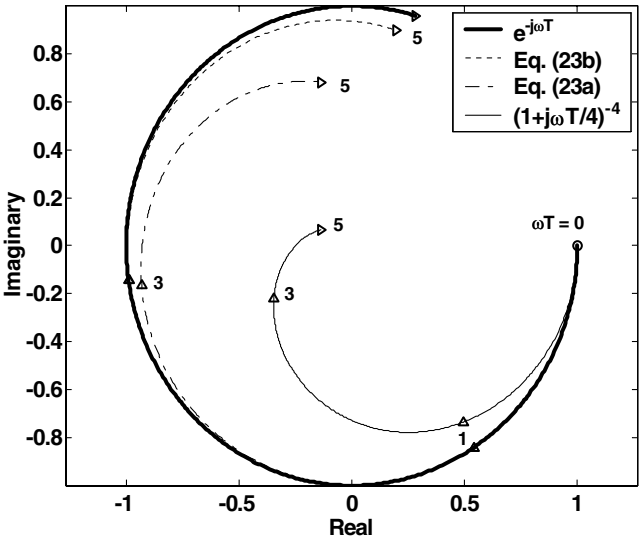

Fig. 2 Various approximations of the gust lag term due to division of the gust force into zones.

The state-space models corresponding to the rational transfer functions Eqs. (23) and (24) could be presented as follows:

$$\{\dot{x}^i_e\} = [A^i_e]\{x^i_e\} + \{B^i_e\} w^{\text{ref}}_G, \qquad w^i_G = [C_e]\{x^i_e\} \tag{27}$$

Here the superscript i indicates that the values of the matrices are the function of the parameter T_i. In Eq. (27)

$$[A^i_e]_{n_e\times n_e} = \begin{bmatrix} \mathbf{0}_{1\times n_e - 1} & \{\bar{A}^i_e\}_{n_e} \\ [I]_{n_e - 1\times n_e - 1} & \end{bmatrix} \tag{28a}$$

$$[C_e]_{1\times n_e} = \begin{bmatrix} \mathbf{0}_{1\times \mathrm{n_e}-1} & -1 \end{bmatrix} \tag{28b}$$

where n_e is the order of the denominator. Then for the third order approximation $n_e = 3$ in Eq. (23a) one obtains

$$\{\bar{A}^i_e\} = -\frac{3}{T_i}\begin{bmatrix} 20T_i^{-2} & 12T_i^{-1} & 3 \end{bmatrix}^T \tag{29a}$$

$$\{B^i_e\} = -\frac{3}{T_i}\begin{bmatrix} 20T_i^{-2} & -8T_i^{-1} & 1 \end{bmatrix}^T \tag{29b}$$

Defining the following functions

$$[Z^{i\sim j}]_{a^{i\sim j}\times(j-i+1)\cdot b} = \begin{bmatrix} [Z^i]_{a_i\times b} & \mathbf{0}_{a_i\times b} & \dots & \mathbf{0}_{a_i\times b} \\ \mathbf{0}_{a_{i+1}\times b} & [Z^{i+1}]_{a_{i+1}\times b} & \dots & \mathbf{0}_{a_{i+1}\times b} \\ \dots & \dots & \dots & \dots \\ \mathbf{0}_{a_j\times b} & \mathbf{0}_{a_j\times b} & \dots & [Z^j]_{a_j\times b} \end{bmatrix} \tag{30a}$$

and

$$\{Z^{i\sim j}\}_{a^{i\sim j}} = \begin{Bmatrix} \{Z^i\}_{a_i} \\ \{Z^i\}_{a_{i+1}} \\ \dots \\ \{Z^i\}_{a_j} \end{Bmatrix} \tag{30b}$$

where

$$a^{i\sim j}=\sum_{l=i}^{j}a_l \tag{31}$$

One can write the system in Eq. (27) as follows:

$$\{\dot{x}_e^{i\sim j}\}_{(j-i+1)\cdot n_e\times 1}=[A_e^{i\sim j}]_{(j-i+1)\cdot n_e\times(j-i+1)\cdot n_e}\{x_e^{i\sim j}\}_{(j-i+1)\cdot n_e\times 1}+\{B_e^{i\sim j}\}_{(j-i+1)\cdot n_e\times 1}w_G^{\mathrm{ref}} \tag{32a}$$

and

$$\{w_G^{i\sim j}\}_{(j-i+1)\cdot n_e\times 1}=[C_e^{i\sim j}]_{(j-i+1)\times(j-i+1)\cdot n_e}\{x_e^{i\sim j}\}_{(j-i+1)\cdot n_e\times 1} \tag{32b}$$

Transformation of the gust lag terms in Eq. (15) from the frequency into the time domain gives

$$[E_G^{\bar{I}}]_{n_{G_{\mathrm{lag}}}^{\bar{I}}\times m}\left\{\frac{\dot{w}_G^{1\sim m}}{V}\right\}_m=\left\{\dot{x}_{G_{\mathrm{lag}}}^{1\sim m}\right\}_{n_{G_{\mathrm{lag}}}^{\bar{I}}}-\frac{V}{b}[R_G^{\bar{I}}]_{n_{G_{\mathrm{lag}}}^{\bar{I}}\times n_{G_{\mathrm{lag}}}^{\bar{I}}}\left\{x_{G_{\mathrm{lag}}}^{1\sim m}\right\}_{n_{G_{\mathrm{lag}}}^{\bar{I}}} \tag{33}$$

Using the gust vector in Eq. (32b) $\{w_G^{1\sim m}\}_{m\cdot n_e\times 1}$, which is related to the first division of the gust force, and substituting it into Eq. (33) one obtains the equation connecting between the gust lag terms with the additional states due to division of the gust into zones

$$\frac{1}{V}[E_G^{\bar{I}}]_{n_{G_{\mathrm{lag}}}^{\bar{I}}\times m}[C_e^{1\sim m}]_{m\times m\cdot n_e}\{\dot{x}_e^{1\sim m}\}_{m\cdot n_e\times 1}=\left\{\dot{x}_{G_{\mathrm{lag}}}^{1\sim m}\right\}_{n_{G_{\mathrm{lag}}}^{\bar{I}}}-\frac{V}{b}[R_G^{\bar{I}}]_{n_{G_{\mathrm{lag}}}^{\bar{I}}\times n_{G_{\mathrm{lag}}}^{\bar{I}}}\left\{x_{G_{\mathrm{lag}}}^{1\sim m}\right\}_{n_{G_{\mathrm{lag}}}^{\bar{I}}} \tag{34}$$

Defining the operator

$$I\equiv 1\sim m \tag{35}$$

and substituting it together with Eq. (32a), the equation above [Eq. (34)] becomes

$$\{\dot{x}_{G_{\mathrm{lag}}}^{I}\}_{n_{G_{\mathrm{lag}}}^{\bar{I}}}=\frac{V}{b}[R_G^{\bar{I}}]_{n_{G_{\mathrm{lag}}}^{\bar{I}}\times n_{G_{\mathrm{lag}}}^{\bar{I}}}\left\{x_{G_{\mathrm{lag}}}^{I}\right\}_{n_{G_{\mathrm{lag}}}^{\bar{I}}}+\frac{1}{V}[E_G^{\bar{I}}]_{n_{G_{\mathrm{lag}}}^{\bar{I}}\times m}[C_e^{I}]_{m\times m\cdot n_e}([A_e^{I}]_{m\cdot n_e\times m\cdot n_e}\{x_e^{I}\}_{m\cdot n_e\times 1}+\{B_e^{I}\}_{m\cdot n_e\times 1}w_G^{\mathrm{ref}}) \tag{36}$$

Similarly, transforming Eq. (16) into the time domain

$$[E_G^{m+1\sim n_G}]_{n_{G_{\mathrm{lag}}}^{m+1\sim n_G}\times n_G-m}\left\{\frac{\dot{w}_G^{m+1\sim n_G}}{V}\right\}_{n_G-m}=\left\{\dot{x}_{G_{\mathrm{lag}}}^{m+1\sim n_G}\right\}_{n_{G_{\mathrm{lag}}}^{m+1\sim n_G}}-\frac{V}{b}[R_G^{m+1\sim n_G}]_{n_{G_{\mathrm{lag}}}^{m+1\sim n_G}\times n_{G_{\mathrm{lag}}}^{m+1\sim n_G}}\left\{x_{G_{\mathrm{lag}}}^{m+1\sim n_G}\right\}_{n_{G_{\mathrm{lag}}}^{m+1\sim n_G}} \tag{37}$$

and substituting Eq. (32) into Eq. (37) leads to the equation that connects the gust lag terms related to the second division of the gust force with the additional states (due to division of the gust into zones)

$$\{\dot{x}_{G_{\mathrm{lag}}}^{II}\}_{n_{G_{\mathrm{lag}}}^{II}}=\frac{V}{b}[R_G^{II}]_{n_{G_{\mathrm{lag}}}^{II}\times n_{G_{\mathrm{lag}}}^{II}}\left\{x_{G_{\mathrm{lag}}}^{II}\right\}_{n_{G_{\mathrm{lag}}}^{II}}+\frac{1}{V}[E_G^{II}]_{n_{G_{\mathrm{lag}}}^{II}\times n_G-m}[C_e^{II}]_{n_G-m\times(n_G-m)\cdot n_e}\times\left([A_e^{II}]_{(n_G-m)\cdot n_e\times(n_G-m)\cdot n_e}\{x_e^{II}\}_{(n_G-m)\cdot n_e\times 1}+\{B_e^{II}\}_{(n_G-m)\cdot n_e\times 1}w_G^{\mathrm{ref}}\right) \tag{38}$$

Here, similar to Eq. (35) the operator II is defined

$$II\equiv m+1\sim n_G \tag{39}$$

The major difference between Eqs. (36–38) is in the system's dimension. For the gusts belonging to the division I, the number of equation is only $n_{G_{\mathrm{lag}}}^{\bar{I}}$, whereas for the division II gust columns the dimension is the sum of the all numbers of the lag terms from $m+1$ up to n_G

$$n_{G_{\mathrm{lag}}}^{II}=n_{G_{\mathrm{lag}}}^{m+1\sim n_G}=\sum_{i=m+1}^{n_G}n_{G_{\mathrm{lag}}}^{i} \tag{40}$$

[see Eq. (31)].

C. White Noise Input and Gust Filters

When the response to random gusts is calculated using LTI state-space models, a gust filter is added to the state-space aeroelastic model to produce the gust input w_G^{ref} due to a white noise input w. The filter is designed to produce a gust input with the desired power spectral density. In the case of the Dryden gust the transfer function is

$$\frac{w_G^{\mathrm{ref}}(s)}{w(s)}=\sigma_{w_G}\frac{\sqrt{3/\tau_G}\,s+\sqrt{1/\tau_G^3}}{[s+(1/\tau_G)]^2} \tag{41}$$

Here σ_{w_G} is a root mean square value (rms) of the gust field vertical velocity. In addition

$$\tau_G=\frac{l_G}{V} \tag{42}$$

where l_G is the scale of turbulence. Because state-space aeroservoelastic models are valid only up to some upper bound on frequencies and to avoid white noise acceleration response of the state-space model due to direct white noise excitation, the low pass filter is added to the gust filter. The transfer function now is modified to be

$$H_G(s)=\frac{a}{s+a}\frac{w_G^{\mathrm{ref}}(s)}{w(s)} \tag{43}$$

The state-space model of this transfer function is now obtained:

$$\{\dot{x}_G\}=[A_G]\{x_G\}+\{B_G\}w,\qquad w_G^{\mathrm{ref}}=[C_G]\{x_G\} \tag{44}$$

where

$$[A_G]_{3\times 3}=\begin{bmatrix}0 & 0 & -a(1/\tau_G^2)\\ 1 & 0 & -(1/\tau_G)[2a+(1/\tau_G)]\\ 0 & 1 & -[a+2(1/\tau_G)]\end{bmatrix},\qquad \{B_G\}_3=a\sigma_{w_G}\begin{Bmatrix}-\sqrt{1/\tau_G^3}\\ -\sqrt{1/\tau_G}\\ 0\end{Bmatrix} \tag{45}$$

D. The Complete State-Space Model

Definition of the new complete state vector in the time domain

$$\{x\}^T=(\{\xi\}^T\ \ \{\dot{\xi}\}^T\ \ \{x_{\mathrm{lag}}\}^T\ \ \{x_{G_{\mathrm{lag}}}^{I}\}^T\ \ \{x_{G_{\mathrm{lag}}}^{II}\}^T\ \ \{x_e\}^T\ \ \{x_G\}^T) \tag{46}$$

finally yields the linear-time-invariant (LTI) state-space open-loop aeroelastic equations of motion

$$\{\dot{x}\}=[L]\{x\}+\{B\}w \tag{47}$$

where

$$[L] = \begin{bmatrix} & \mathbf{0}_{n\times n_{G_{lag}}^{\bar{I}}} & \mathbf{0}_{n\times n_{G_{\text{lag}}}^{II}} & \mathbf{0}_{n\times n_G\cdot n_e} & \mathbf{0}_{n\times 3} \\ [L_s] & [L_D^{\bar{I}}] & [L_D^{II}] & [L_{e_1}] & [L_{G_1}] \\ & \mathbf{0}_{n_{\text{lag}}\times n_{G_{\text{lag}}}^{\bar{I}}} & \mathbf{0}_{n_{\text{lag}}\times n_{G_{\text{lag}}}^{II}} & \mathbf{0}_{n_{\text{lag}}\times n_G\cdot n_e} & \mathbf{0}_{n_{\text{lag}}\times 3} \\ \mathbf{0}_{n_{G_{\text{lag}}}^{\bar{I}}\times 2n+n_{\text{lag}}} & \frac{V}{b}[R_G^{\bar{I}}] & \mathbf{0}_{n_{G_{\text{lag}}}^{\bar{I}}\times n_{G_{\text{lag}}}^{II}} & [L_{e_2}] & [L_{G_2}] \\ \mathbf{0}_{n_{G_{\text{lag}}}^{II}\times 2n+n_{\text{lag}}} & \mathbf{0}_{n_{G_{\text{lag}}}^{II}\times n_{G_{\text{lag}}}^{\bar{I}}} & \frac{V}{b}[R_G^{II}] & [L_{e_3}] & [L_{G_3}] \\ \mathbf{0}_{n_G\cdot n_e\times 2n+n_{\text{lag}}} & \mathbf{0}_{n_G\cdot n_e\times n_{G_{\text{lag}}}^{\bar{I}}} & \mathbf{0}_{n_G\cdot n_e\times n_{G_{\text{lag}}}^{II}} & [A_e^{1n_G}] & [L_{G_4}] \\ \mathbf{0}_{3\times 2n+n_{\text{lag}}} & \mathbf{0}_{3\times n_{G_{\text{lag}}}^{\bar{I}}} & \mathbf{0}_{3\times n_{G_{\text{lag}}}^{II}} & \mathbf{0}_{3\times n_G\cdot n_e} & [A_G] \end{bmatrix} \tag{48}$$

and

$$\{B\} = \begin{Bmatrix} \mathbf{0}_{2n+n_{\text{lag}}+n_{G_{\text{lag}}}^{\bar{I}}+n_{G_{\text{lag}}}^{II}+n_G\cdot n_e} \\ \{B_G\}_3 \end{Bmatrix} \tag{49}$$

In Eq. (48) $[L_s]$ is the part of the system's matrix that is not influenced by gust states.

$$[L_s]_{2n+n_{\text{lag}}\times 2n+n_{\text{lag}}} = \begin{bmatrix} \mathbf{0}_{n\times n} & [I]_{n\times n} & \mathbf{0}_{n\times n_{\text{lag}}} \\ -([\bar{M}]^{-1}[\bar{K}])_{n\times n} & -([\bar{M}]^{-1}[\bar{C}])_{n\times n} & q_D[\bar{M}]^{-1}_{n\times n}[D]_{n\times n_{\text{lag}}} \\ \mathbf{0}_{n_{\text{lag}}\times n} & [E]_{n_{\text{lag}}\times n} & \frac{V}{b}[R]_{n_{\text{lag}}\times n_{\text{lag}}} \end{bmatrix} \tag{50}$$

The rest of the matrices in Eq. (48) are due to the gust excitation and defined as follows:

$$[L_D^{\bar{I}}] = q_D[\bar{M}]^{-1}[D_G^{\bar{I}}] \tag{51a}$$

$$[L_D^{II}]_{n\times n_{G_{\text{lag}}}^{II}} = q_D[\bar{M}]^{-1}\begin{bmatrix} [D_G^{m+1}] & [D_G^{m+2}] & \dots & [D_G^{n_G}] \end{bmatrix} \tag{51b}$$

$$[L_{e_1}]_{n\times n_G\cdot n_e} = \frac{q_D}{V}[\bar{M}]^{-1}\left([A_{G_0}][C_e^{1\sim n_G}] + \frac{b}{V}[A_{G_1}][C_e^{1\sim n_G}][A_e^{1\sim n_G}]\right) \tag{52a}$$

$$[L_{e_2}]_{n_{G_{\text{lag}}}^{\bar{I}}\times n_G\cdot n_e} = \frac{1}{V}\begin{bmatrix} ([E_G^{\bar{I}}][C_e^I][A_e^I])_{n_{G_{\text{lag}}}^{\bar{I}}\times m\cdot n_e} & \mathbf{0}_{n_{G_{\text{lag}}}^{\bar{I}}\times(n_G-m)n_e} \end{bmatrix} \tag{52b}$$

$$[L_{e_3}]_{n_{G_{\text{lag}}}^{II}\times n_G\cdot n_e} = \frac{1}{V}\begin{bmatrix} 0_{n_{G_{\text{lag}}}^{II}\times m\cdot n_e} & ([E_G^{II}][C_e^{II}][A_e^{II}])_{n_{G_{\text{lag}}}^{II}\times(n_G-m)n_e} \end{bmatrix} \tag{52c}$$

$$[L_{G_1}]_{n\times 3} = q_D\frac{b}{V^2}[\bar{M}]^{-1}[A_{G_1}][C_e^{1\sim n_G}]\{B_e^{1\sim n_G}\}[C_G] \tag{53a}$$

$$[L_{G_2}]_{n_{G_{\text{lag}}}^{\bar{I}}\times 3} = \frac{1}{V}[E_G^{\bar{I}}][C_e^I]\{B_e^I\}[C_G] \tag{53b}$$

$$[L_{G_3}]_{n_{G_{\text{lag}}}^{II}\times 3} = \frac{1}{V}[E_G^{II}][C_e^{II}]\{B_e^{II}\}[C_G] \tag{53c}$$

$$[L_{G_4}]_{n_G\cdot n_e\times 3} = \{B_e^{1\sim n_G}\}[C_G] \tag{53d}$$

The matrices $[A_e^{1\sim n_G}]_{n_G\cdot n_e\times n_G\cdot n_e}$ and $[C_e^{1\sim n_G}]_{n_G\times n_G\cdot n_e}$ are created using the function in Eq. (30a), and

$$\{B_e^{1\sim n_G}\} = \{B_e^{1\sim n_G}\}_{n_G\cdot n_e\times 1}$$

is generated through the function in Eq. (30b).

Based on Eq. (47) for the open-loop case, the covariance matrix of the state vector $\{x\}$ for the case of stationary white noise excitation can be found by solving an algebraic Lyapunov equation [7]:

$$[L][X] + [X][L]^T = -\{B\}\{B\}^T \tag{54}$$

E. Sensitivity Analysis

Sensitivity analysis of the aeroelastic LTI system matrix with respect to some design variable DV involves the differentiation of the MIST approximation [Eqs. (2), (9), and (10)]. The MIST approximation generation process is nonlinear and involves an iterative process. The problem of obtaining derivatives of the MIST approximants in the case where aerodynamic forces change due to shape variation of a configuration was addressed in a previous work [3]. By conducting an investigation based on singular value decomposition of Roger approximants, the authors of [3] obtain the connection between Roger and MIST approximations, showing that approximate sensitivities of MIST rational approximations can be calculated without a nonlinear iterative process as follows by holding the $[D]$ matrix frozen:

$$\left[\frac{\partial Q(jk)}{\partial DV}\right] \approx \left[\frac{\partial A_0}{\partial DV}\right] + jk\left[\frac{\partial A_1}{\partial DV}\right] + (jk)^2\left[\frac{\partial A_2}{\partial DV}\right] + [D]jk([I]k - [R]^{-1})\left[\frac{\partial E}{\partial DV}\right] \tag{55}$$

The derivative of the static aerodynamic stiffness matrix is calculated using the steady state aerodynamic matrix $[Q]$:

$$\left[\frac{\partial A_0}{\partial DV}\right] = \left[\frac{\partial Q(k=0)}{\partial DV}\right]$$

Thus Eq. (55) is now a linear equation for $[\partial A_1/\partial DV]$, $[\partial A_2/\partial DV]$, and $[\partial E/\partial DV]$, and it is solved by a single least-squares step without iterations. With MIST approximant and its sensitivities available at some reference design point (REF), approximations of the MIST matrices away from that reference point can be obtained using direct or reciprocal Taylor series. In the case of direct approximation

$$[A_i] \approx [A_i]_{\text{REF}} + \sum_j \left[\frac{\partial A_i}{\partial DV_j}\right]\Bigg|_{\text{REF}}(DV_j - DV_{j_{\text{REF}}}), \qquad (i = 0, 1, 2) \tag{56}$$

$$[E] \approx [E]_{\text{REF}} + \sum_j \left[\frac{\partial E}{\partial DV_j}\right]\Bigg|_{\text{REF}}(DV_j - DV_{j_{\text{REF}}}) \tag{57}$$

$$[D] \approx [D]_{\text{REF}} \tag{58}$$

Equations (55–58) apply to the generalized aerodynamic terms due to motion in the structural modes used. For the gust terms the relations are similar. However, it is preferable in the gust MIST case to keep the matrix $[E]$ as a constant and allow $[D]$ to vary, because the dimension of $[E]$, $(n_{G_{\text{lag}}}^{\bar{I}} \times m)$, in the majority of cases is lower than the dimension of the matrix $[D_G^{\bar{I}}]_{n\times n_{G_{\text{lag}}}^{\bar{I}}}$. In this way the precision of the derivatives of the MIST approximation will be higher, because more terms in the sensitivity-based approximation are allowed to change

$$\left[\frac{\partial Q_G^{\bar{I}}}{\partial DV}\right] \approx \left[\frac{\partial A_{G_0}^{\bar{I}}}{\partial DV}\right] + jk\left[\frac{\partial A_{G_1}^{\bar{I}}}{\partial DV}\right] + jk\left[\frac{\partial D_G^{\bar{I}}}{\partial DV}\right]\left(jk[I] - \frac{V}{b}[R_G^{\bar{I}}]\right)^{-1}[E_G^{\bar{I}}] \tag{59}$$

and similarly for the II gust inputs division

$$\left\{\frac{\partial Q_G^i}{\partial DV}\right\} \approx \left\{\frac{\partial A_{G_0}^i}{\partial DV}\right\} + jk\left\{\frac{\partial A_{G_1}^i}{\partial DV}\right\} + jk\left[\frac{\partial D_G^i}{\partial DV}\right](jk[I] - [R_G^i])^{-1}\{E_G^i\}, \qquad i = m+1, \ldots, n_G \tag{60}$$

Now sensitivities for the complete system's model can be found by differentiating Eqs. (48–54) as follows:

$$\left[\partial L/\partial DV\right] = \begin{bmatrix} & \mathbf{0}_{n\times n_{G_{\text{lag}}}^{\bar{I}}} & \mathbf{0}_{n\times n_{G_{\text{lag}}}^{II}} & \mathbf{0}_{n\times n_G\cdot n_e} & \mathbf{0}_{n\times 3} \\ \left[\partial L_s/\partial DV\right] & \left[\partial L_D^{\bar{I}}/\partial DV\right]_{n\times n_{G_{\text{lag}}}^{\bar{I}}} & \left[\partial L_D^{II}/\partial DV\right]_{n\times n_{G_{\text{lag}}}^{II}} & \left[\partial L_{e_1}/\partial DV\right] & \left[\partial L_{G_1}/\partial DV\right] \\ & \mathbf{0}_{n_{\text{lag}}\times n_{G_{\text{lag}}}^{\bar{I}}} & \mathbf{0}_{n_{\text{lag}}\times n_{G_{\text{lag}}}^{II}} & \mathbf{0}_{n_{\text{lag}}\times n_G\cdot n_e} & \mathbf{0}_{n_{\text{lag}}\times 3} \\ \mathbf{0}_{n_{G_{\text{lag}}}^{\bar{I}}\times 2n+n_{\text{lag}}} & \mathbf{0}_{n_{G_{\text{lag}}}^{\bar{I}}\times n_{G_{\text{lag}}}^{\bar{I}}} & \mathbf{0}_{n_{G_{\text{lag}}}^{\bar{I}}\times n_{G_{\text{lag}}}^{II}} & \left[\partial L_{e_2}/\partial DV\right] & \left[\partial L_{G_2}/\partial DV\right] \\ \mathbf{0}_{n_{G_{lag}}^{II}\times 2n+n_{\text{lag}}} & \mathbf{0}_{n_{G_{\text{lag}}}^{II}\times n_{G_{\text{lag}}}^{\bar{I}}} & \mathbf{0}_{n_{G_{\text{lag}}}^{II}\times n_{G_{\text{lag}}}^{II}} & \left[\partial L_{e_3}/\partial DV\right] & \left[\partial L_{G_3}/\partial DV\right] \\ \mathbf{0}_{n_G\cdot n_e\times 2n+n_{\text{lag}}} & \mathbf{0}_{n_G\cdot n_e\times n_{G_{\text{lag}}}^{\bar{I}}} & \mathbf{0}_{n_G\cdot n_e\times n_{G_{\text{lag}}}^{II}} & \left[\partial A_e^{1\sim n_G}/\partial DV\right] & \left[\partial L_{G_4}/\partial DV\right] \\ \mathbf{0}_{3\times 2n+n_{\text{lag}}} & \mathbf{0}_{3\times n_{G_{\text{lag}}}^{\bar{I}}} & \mathbf{0}_{3\times n_{G_{\text{lag}}}^{II}} & \mathbf{0}_{3\times n_G\cdot n_e} & \mathbf{0}_{3\times 3} \end{bmatrix} \tag{61}$$

The values of the vector $\{B\}$ do not depend on any shape parameter, therefore

$$\left\{\frac{\partial B}{\partial DV}\right\} = \{\mathbf{0}_{2n+n_{\text{lag}}+n_{G_{\text{lag}}}^{\bar{I}}+n_{G_{\text{lag}}}^{II}+n_G\cdot n_e+3}\} \tag{62}$$

The derivative of the part of the system's matrix corresponding to structural motions, followed by Eq. (55) is

$$\left[\frac{\partial L_s}{\partial DV}\right] = \begin{bmatrix} 0 & 0 & 0 \\ -[\partial([\bar{M}]^{-1}[\bar{K}])/\partial DV] & -[\partial([\bar{M}]^{-1}[\bar{C}])/\partial DV] & q_D(\partial[\bar{M}]^{-1}/\partial DV)[D] \\ 0 & \left[\partial E/\partial DV\right] & 0 \end{bmatrix} \tag{63}$$

The derivatives of the matrices $[\bar{M}]$, $[\bar{C}]$, and $[\bar{K}]$ are obtained as follows:

$$\left[\frac{\partial \bar{M}}{\partial DV}\right] = \left[\frac{\partial M}{\partial DV}\right] - q_D\frac{b^2}{V^2}\left[\frac{\partial A_2}{\partial DV}\right], \qquad \left[\frac{\partial \bar{K}}{\partial DV}\right] = \left[\frac{\partial K}{\partial DV}\right] - q_D\left[\frac{\partial A_0}{\partial DV}\right], \qquad \left[\frac{\partial \bar{C}}{\partial DV}\right] = \left[\frac{\partial C}{\partial DV}\right] - q_D\frac{b}{V}\left[\frac{\partial A_1}{\partial DV}\right] \tag{64}$$

The rest of the derivatives are

$$\left[\frac{\partial L_D^{\bar{I}}}{\partial DV}\right]_{n\times n_{G_{\text{lag}}}^{\bar{I}}} = q_D\left(\frac{\partial[\bar{M}]^{-1}}{\partial DV}D_G^{\bar{I}} + [\bar{M}]^{-1}\left[\frac{\partial D_G^{\bar{I}}}{\partial DV}\right]\right) \tag{65a}$$

$$\left[\frac{\partial L_D^{II}}{\partial DV}\right]_{n\times n_{G_{\text{lag}}}^{II}} = q_D\frac{\partial[\bar{M}]^{-1}}{\partial DV}\left[\,[D_G^{m+1}] \quad [D_G^{m+2}] \quad \ldots \quad [D_G^{n_G}]\,\right] + q_D[\bar{M}]^{-1}\left[\left[\frac{\partial D_G^{m+1}}{\partial DV}\right] \quad \left[\frac{\partial D_G^{m+2}}{\partial DV}\right] \quad \ldots \quad \left[\frac{\partial D_G^{n_G}}{\partial DV}\right]\right] \tag{65b}$$

$$\left[\frac{\partial L_{e_1}}{\partial DV}\right]_{n\times n_G\cdot n_e} = \frac{q_D}{V}\left[\frac{\partial A_{G_0}}{\partial DV}\right][C_e^{1\sim n_G}] + q_D\frac{b}{V^2}\left(\left[\frac{\partial A_{G_1}}{\partial DV}\right][C_e^{1\sim n_G}][A_e^{1\sim n_G}] + [A_{G_1}][C_e^{1\sim n_G}]\left[\frac{\partial A_e^{1\sim n_G}}{\partial DV}\right]\right) \tag{66a}$$

$$\left[\frac{\partial L_{e_2}}{\partial DV}\right]_{n_{G_{\text{lag}}}^{\bar{I}}\times n_G\cdot n_e} = \frac{1}{V}\left[\,[E_G^{\bar{I}}][C_e^I]\left[\frac{\partial A_e^I}{\partial DV}\right] \quad \mathbf{0}_{n_{G_{\text{lag}}}^{\bar{I}}\times(n_G-m)n_e}\,\right] \tag{66b}$$

$$\left[\frac{\partial L_{e_3}}{\partial DV}\right]_{n_{G_{\text{lag}}}^{II}\times n_G\cdot n_e} = \frac{1}{V}\left[\,\mathbf{0}_{n_{G_{\text{lag}}}^{II}\times m\cdot n_e} \quad [E_G^{II}][C_e^{II}]\left[\frac{\partial A_e^{II}}{\partial DV}\right]\,\right] \tag{66c}$$

$$\left[\frac{\partial L_{G_1}}{\partial DV}\right]_{n\times 3} = q_D\frac{b}{V^2}\left(\left[\frac{\partial A_{G_1}}{\partial DV}\right][C_e^{1n_G}]\{B_e^{1\sim n_G}\} + [A_{G_1}][C_e^{1\sim n_G}]\left\{\frac{\partial B_e^{1\sim n_G}}{\partial DV}\right\}\right)[C_G] \tag{67a}$$

$$\left[\frac{\partial L_{G_2}}{\partial DV}\right]_{n_{G_{\text{lag}}}^{\bar{I}}\times 3} = \frac{1}{V}[E_G^{\bar{I}}][C_e^I]\left\{\frac{\partial B_e^I}{\partial DV}\right\}[C_G] \tag{67b}$$

$$\left[\frac{\partial L_{G_3}}{\partial DV}\right]_{n_{G_{\text{lag}}}^{II}\times 3} = \frac{1}{V}[E_G^{II}][C_e^{II}]\left\{\frac{\partial B_e^{II}}{\partial DV}\right\}[C_G] \tag{67c}$$

$$\left[\frac{\partial L_{G_4}}{\partial DV}\right]_{n_G\cdot n_e\times 3} = \left\{\frac{\partial B_e^{1\sim n_G}}{\partial DV}\right\}[C_G] \tag{67d}$$

In Eqs. (66) and (67) the derivatives of the of the vectors $\{\partial B_e^I/\partial DV\}$, $\{\partial B_e^{II}/\partial DV\}$, $\{\partial B_e^{1\sim n_G}/\partial DV\}$ and the matrices $[\partial A_e^I/\partial DV]$, $[\partial A_e^{II}/\partial DV]$, $[\partial A_e^{1\sim n_G}/\partial DV]$ are the functions [Eqs. (27) and (28)] of $\{\partial B_e^i/\partial DV\}$ and $[\partial A_e^i/\partial DV]$ where

$$\left[\frac{\partial A_e^i}{\partial DV}\right]_{n_e\times n_e} = \left[\mathbf{0}_{n_e\times n_e-1} \quad \left\{\frac{\partial \bar{A}_e^i}{\partial DV}\right\}_{n_e}\right] \tag{68}$$

The vectors $\{\partial \bar{A}_e^i/\partial DV\}$ and $\{\partial B_e^i/\partial DV\}$ are found by differentiating Eq. (29)

$$\left\{\frac{\partial \bar{A}_e^i}{\partial DV}\right\} = \frac{9}{T_i^2}\frac{\partial T_i}{\partial DV}\left[\,20T_i^{-2} \quad 8T_i^{-1} \quad 1\,\right]^T \tag{69}$$

$$\left\{\frac{\partial B_e^i}{\partial DV}\right\} = \frac{3}{T_i^2}\frac{\partial T_i}{\partial DV}\left[\,60T_i^{-2} \quad 16T_i^{-1} \quad 1\,\right]^T \tag{70}$$

It is important to note that in the sensitivity equations for the gust terms changes are accounted for not only due to the change in size and locations of aerodynamic panels (and the resulting change in aerodynamic influence coefficients) but also changes in the relative locations of gust input reference points corresponding to different gust input zones.

Sensitivity of the state covariance matrix with respect to shape design variables is obtained by differentiation of Eq. (54):

$$[L]\left[\frac{\partial X}{\partial DV}\right] + \left[\frac{\partial X}{\partial DV}\right][L]^T = -\left[\frac{\partial L}{\partial DV}\right][X] - [X]\left[\frac{\partial L}{\partial DV}\right]^T \tag{71}$$

This sensitivity equation is another Lyapunov equation with similar system matrices on the left hand side, and with a new right hand side for every design variable. Because the original Lyapunov equation for state covariance has been already solved during the analysis step, matrices are already decomposed and solutions of the equation for additional right hand sides are obtained quickly.

Whether gust responses (deformations and stresses) to time dependent gust excitation or random gust excitation are required, sensitivity of those responses with respect to configuration shape DVs can be obtained once the derivatives of the system's matrices are obtained based on the method outlined above.

III. Variable Shape Wing-Tail Test Case

The wing/horizontal tail (wing-tail) configuration shown in Fig. 3 is used to evaluate the sensitivities and approximations presented here. The half-span length of the wing and horizontal tail are $Y_w = 18$ m and $Y_t = 7$ m, respectively. Their root-chord lengths are $b_{\text{wr}} = 2b = 9$ m and $b_{\text{tr}} = 4$ m, and their root's leading edge locations are 24 and 46 m, respectively, measured from the nose. The wing's tip chord length is $b_{\text{wt}} = 3$ m and the tail's tip chord is $b_{\text{tt}} = 2$ m.

The fuselage is modeled only for structural analysis as a group of connected beam elements with the total length of 50 m. The sweep angle of the wings is Δ (which is a shape design variable DV), and it varies from 0 to 30 deg. The wings and the horizontal tail are assumed to have a thickness of $t = 0.08$ m and their structural material characteristics are the following: $E = 73.8$ GPa, $G = 24.4$ GPa, and $\rho = 2540$ kg/m^3.

The structural finite element results for the configuration for the different values of the sweep angle Δ were calculated using MSC NASTRAN [8]. The first 18 modes (including the pitch rigid body mode) are taken for the aeroelastic analysis using Mach = 0 aerodynamics produced by the ZAERO code [9]. The generalized aerodynamic force coefficient matrix corresponding to structural mode shapes is approximated using $n_{\text{lag}} = 10$ lag terms. The configuration is divided into three different gust zones $n_G = 3$. The reference point for the whole configuration (where the gust wave starts) is kept at the nose $x_{\text{ref}} = 0$, thus the distances of the other gust reference points are $L_2 = 46$ m and $L_3 = 24$ m [see Eq. (21)]. L_1 is a function of the sweep angle

$$L_1 = 27 + \tfrac{1}{2}Y_w \tan(\Delta) \tag{72}$$

and therefore varies with the shape changes of the configuration.

The first gust input zone (as shown in Fig. 3) includes the panels on the outer half of the wing and it is approximated together with the gust aerodynamics of the horizontal tail (the second gust zone) using $n^I_{G_{\text{lag}}} = 8$ lag terms. The inner half of the wing, which belongs to the third gust zone, is approximated separately with $n^{II}_{G_{\text{lag}}} = n^3_{G_{\text{lag}}} = 8$ lag terms as well. Such an arrangement is selected based on the behavior of the gust aerodynamic force coefficient matrix. As shown in Figs. 4a and 4b the behavior of the aerodynamic terms of the first $[Q^I_{G_{41}}(k) \equiv Q^1_{G_4}(k)$; see Eqs. (8) and (9)] and the second $[Q^I_{G_{42}}(k) \equiv Q^2_{G_4}(k)]$ gust zones (as functions of reduced frequency) is similar, whereas the third gust zone $[Q^{II}_{G_{41}}(k) \equiv Q^3_{G_4}(k)$—see Eq. (10)] is characterized by spiral behavior [Fig. 4c]. The division into zones, as was mentioned before, solves the problem of the highly spiraled behavior of the gust aerodynamics (as for the outer wing zone and the horizontal tail). To eliminate the remaining spiral behavior in the third zone one needs to introduce additional gust zones within the inner half of the wing. However, as shown in Fig. 4c, this is unnecessary in the present case because its aerodynamic matrix is well approximated using a separate MIST approximant that manages, using 8 dedicated lag terms, to capture the behavior.

Although methods for the unsteady aerodynamic analytic sensitivity evaluation for variable shape configurations have been developed [10], no such general capability yet exists. The planform shape design sensitivities of the unsteady aerodynamic forces $[Q(jk)]$ and $[Q_G(jk)]$ are calculated here using finite differences applied on the results of the ZAERO code.

The reference sweep angle is chosen $\Delta_{\text{REF}} = 15$ deg with 1% perturbation $d\Delta = 0.15$ deg for finite differences. Shape sensitivities of the minimum-state approximation are calculated analytically, using the method in Eqs. (55–60), and Taylor series approximations of the aerodynamic matrices are constructed [using Eqs. (56–58)]. The sensitivities of the state-space model then can be obtained analytically through Eqs. (61–70).

The example of the covariance of generalized state vector term related to the third structural mode is presented in Fig. 5. The dots are "exact" results obtained [solving the Lyapunov equation (54)] by repeated full analyses using NASTRAN, ZAERO, MIST codes and state-space stability analyses for each geometric shape (every 5 deg from 0 to 30 deg). Approximate results using the sensitivities of the system's matrices are obtained by solving Eq. (54) with new state-space matrices $[L]$ [Eq. (47)] approximated as follows:

$$[L] = [L]_{\Delta_{\text{REF}}} + \left[\frac{\partial L}{\partial \Delta}\right]_{\Delta_{\text{ref}}} (\Delta - \Delta_{\text{REF}}) \tag{73}$$

The $[B]$ matrix does not depend on the sweep angle and then remains constant. The difference between the solid and the dashed lines is in

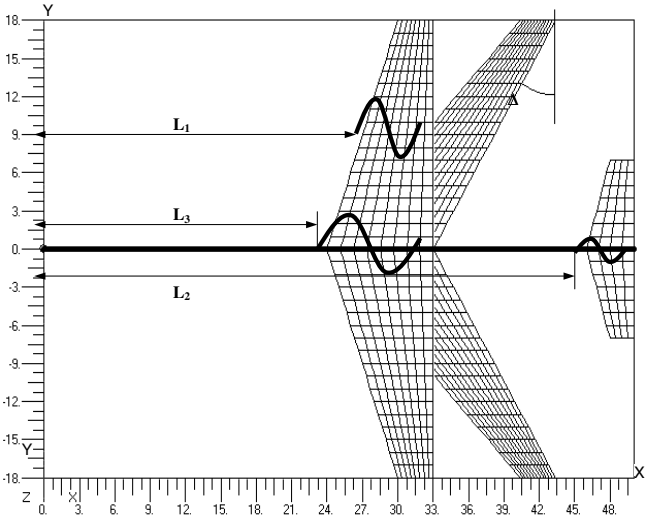

Fig. 3 The wing-tail model with 3 gust zones. Planform shape variations of the wing are shown.

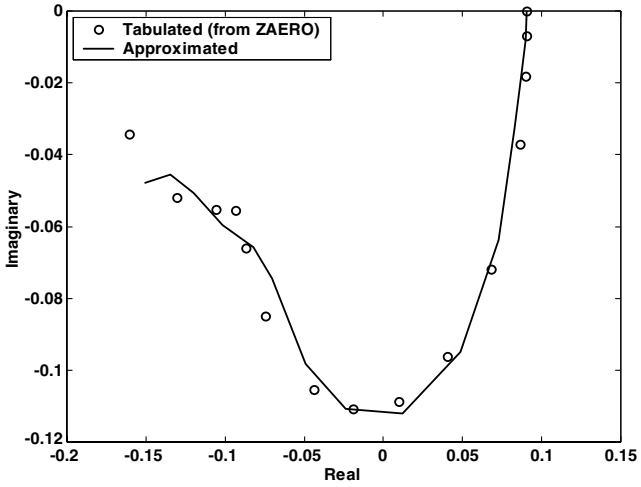

a)

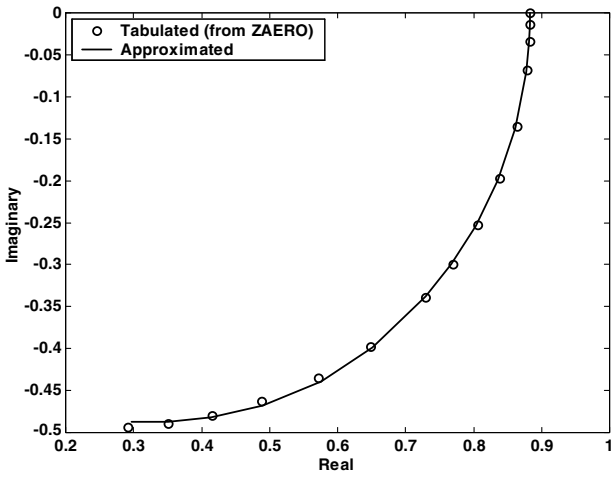

b)

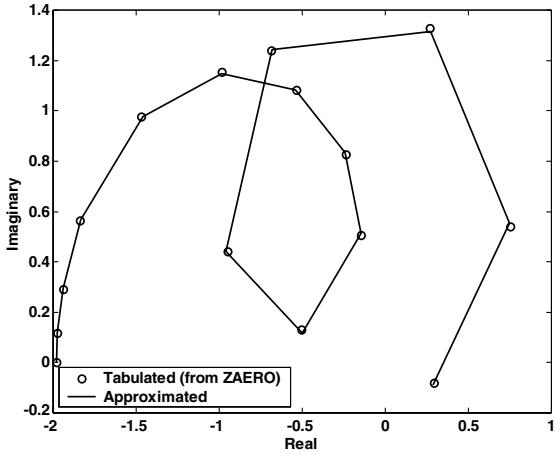

c)

Fig. 4 Quality of MIST approximation for gust terms with $n^{\bar{I}}_{G_{\text{lag}}} = 8$ and $n^{II}_{G_{\text{lag}}} = n^{\bar{3}}_{G_{\text{lag}}} = 8$ (in case of $V = 75$ m/sec and $\Delta = 15$ deg). a) Matching the $Q^{\bar{I}}_{G_{41}}(k)$ term; b) Matching the $Q^{\bar{I}}_{G_{42}}(k)$ term; c) Matching the $Q^{II}_{G_{41}}(k)$ term.

the method of calculating the sensitivity of the state-space matrix

$$\left[\frac{\partial L}{\partial \Delta}\right]_{\Delta_{\text{REF}}}$$

The solid line represents the results calculated based on analytical

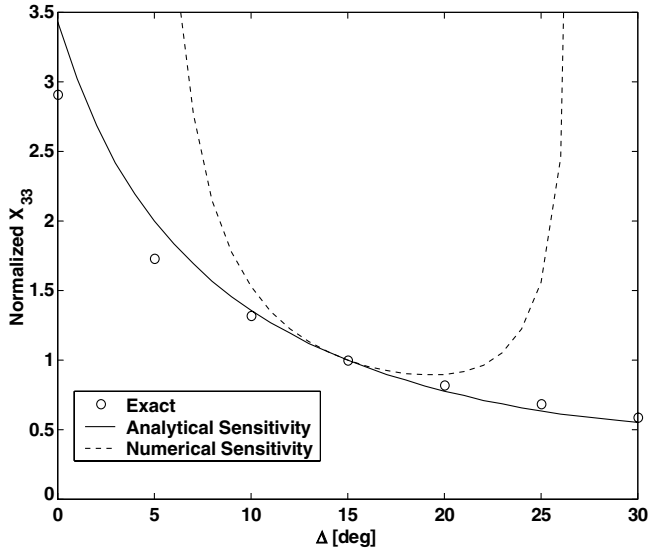

Fig. 5 Comparison between the sensitivity methods based on analytical and numerical derivatives (for $V = 75$ m/sec).

sensitivities of the coefficients of the matrix

$$\left[\frac{\partial L}{\partial \Delta}\right]_{\Delta_{\text{REF}}}$$

using Eqs. (55–70), whereas the dashed line follows the results of the numerical, finite differences method sensitivities. These results are obtained by directly calculating the above matrix using finite differences:

$$\left[\frac{\partial L}{\partial \Delta}\right]_{\Delta_{\text{REF}}} = \frac{[L]_{\Delta_{\text{REF}}+d\Delta} - [L]_{\Delta_{\text{REF}}}}{d\Delta} \tag{74}$$

(As mentioned above, the results of the both methods for $[\partial L/\partial \Delta]_{\Delta_{\text{REF}}}$ then used in Eq. (73) to approximate the new state-space matrix and then solve the Lyapunov Eq. (54) for each method, to obtain the covariance matrix $[X]$.)

It is obvious from the figure that the analytical sensitivities give much better results in wider range of Δ (the maximum deviation in the whole range of the sweep angle $0 \text{ deg} < \Delta < 30 \text{ deg}$ is 15% at $\Delta = 0$ deg). The numerical sensitivity can be used only in the small range of $\sim 8 \text{ deg} < \Delta < \sim 22$ deg with the same maximal error of 15%.

In addition to the fact that the analytical sensitivities provide good results, the method is very efficient in terms of calculation time, compared with the time needed to run the repeated full analyses. With 344 aerodynamic panels for the wing-tail configuration shown in Fig. 3, it takes more than 10 min to a 1.6 GHz Pentium IV processor to run the full analysis for a single sweep angle value of the wing. On the other hand, the sensitivity analysis run (based on the results for the reference point) takes only a few seconds. Besides the significant reduction at the CPU time, the user saves the time and effort needed to generate finite element and aerodynamic models at each point (other than the reference and the perturbated design points).

Figure 6 shows the flutter speed versus the sweep angle of the wing. The results of the exact solution of the state-space model coincide in almost the entire range of Δ with those of the ZAERO g-method. This demonstrates the high quality match of the aerodynamic force coefficients by MIST approximation. The results based on the sensitivity Eq. (73) follow the behavior of the exact solution with maximum error of less than 8% at the sweep angle of 5 deg.

Figure 7 presents the change in the damping coefficient at first 3 modes as a function of the sweep angle. The damping ratio is obtained from the complex poles as

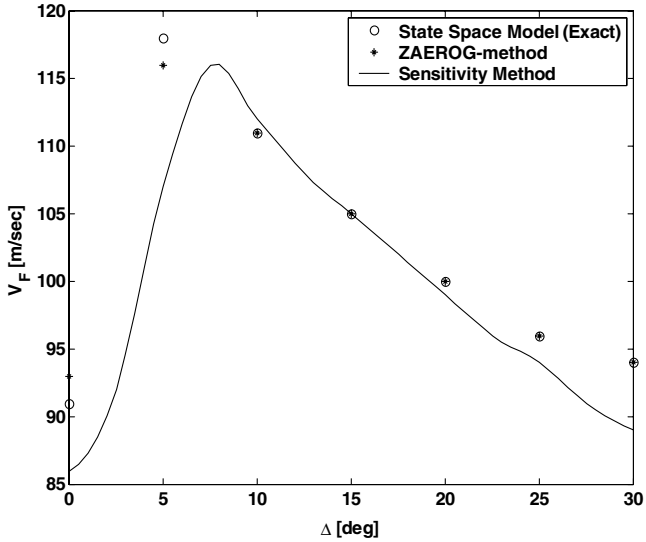

Fig. 6 Flutter speed of the wing-tail configuration as a function of the sweep angle of the wing.

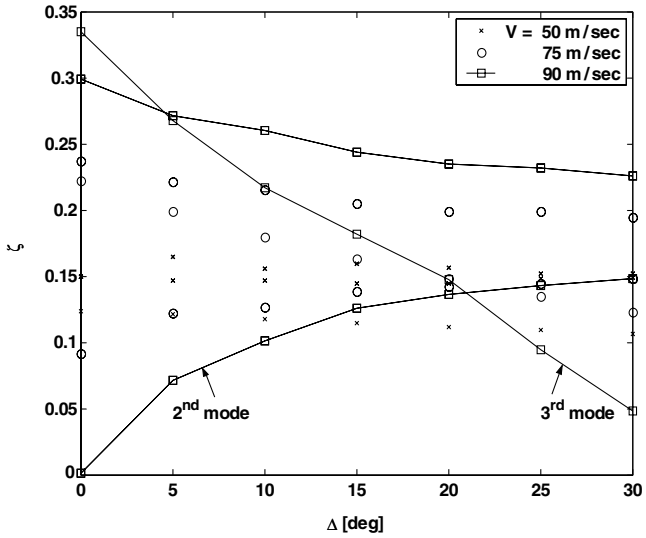

Fig. 7 Map of the damping coefficient at low frequencies as a function of the sweep angle and the speed of flight.

$$\zeta = -\frac{\mathrm{Im}(\lambda)}{\sqrt{\mathrm{Re}^2(\lambda) + \mathrm{Im}^2(\lambda)}} \tag{75}$$

and it is also a function of the flight velocity. As the sweep angle varies flutter mechanisms change not only due to structural and aerodynamic variation of the moving segments but also through varying levels of wing/tail aerodynamic interference. Above $\Delta > \sim 10$ deg system response becomes more dominated by the frequency close to the natural frequency of the third mode, as shown in Fig. 7, compared with the effects of the second mode earlier.

Figure 8 shows the response of the system to white noise. The covariance of a displacement in z direction

$$\sigma_z^2 = E[[\Phi]_z\{\xi\}([\Phi]_z\{\xi\})^T] = E[[\Phi]_z\{\xi\}\{\xi\}^T[\Phi]_z^T]$$
$$= [\Phi]_z E[\{\xi\}\{\xi\}^T][\Phi]_z^T \tag{76}$$

where $[\Phi]_z$ is the eigenvector contribution at the z direction calculated at two test points: the wing tip and the tail tip. The solid line presents the results obtained by solving Eqs. (54) and (76) using the approximated state matrix $[L]$ [Eq. (73)]. On the other hand the dashed line is constructed using the solution in Eq. (71) [together

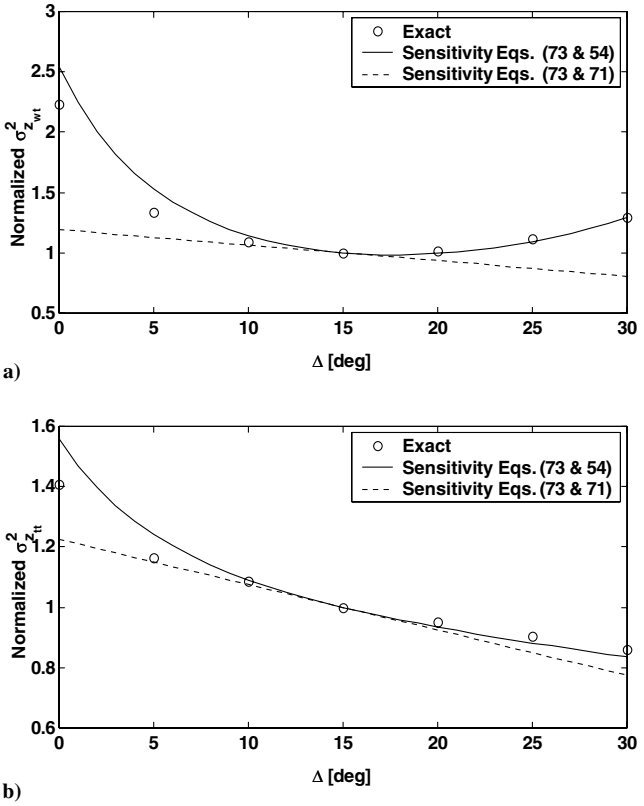

Fig. 8 Normalized covariance of the a) wings tip and b) tails tip deflections for various sweep angles and its comparison using exact analysis and sensitivity methods.

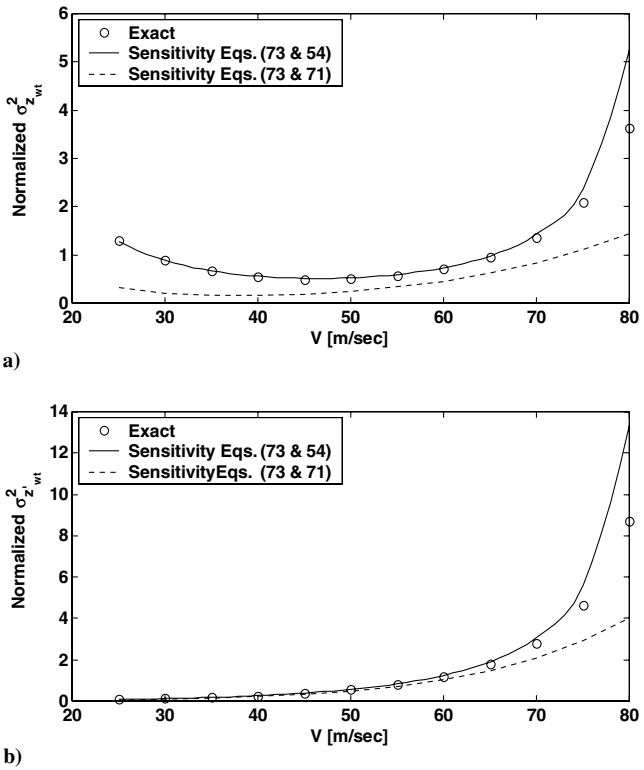

Fig. 9 Comparison of the exact analysis versus sensitivity methods for the normalized covariance of the wings tip a) deflection b) velocity as a function of the speed of flight ($\Delta = 0$ deg) (The reference point for this approximation is at sweep angle of 15 deg.)

with Eq. (76)] in the following first order Taylor series approximation:

$$\sigma_z^2 = \sigma_z^2|_{\Delta_{\mathrm{REF}}} + \frac{\partial}{\partial \Delta}([\Phi]E[\{\xi\}\{\xi\}^T][\Phi]_z^T)|_{\Delta_{\mathrm{REF}}}(\Delta - \Delta_{\mathrm{REF}})$$

and therefore has a constant slope. This approximation can follow with better precision only a monotonic behavior [see Fig. 8b], however, due to nonmonotonic flutter velocity the covariance of the motions at the wings tip rises at both 0 and 30 deg sweep angles.

The approximation based on Eqs. (54), (73), and (76) provides a good match to the exact solution and in most of the range of sweep angles the error is less than 5%, with an exception of the vicinity of $\Delta = 0$ deg where the error reaches to 12%. One of the reasons for this is that the 0 deg sweep angle reflects a 100% change of the design variable from its initial point. But the main reason is that at 0 deg sweep angle the configuration first reaches instability and thus damping variation in the critical pole leads to sensitivity of the gust response rms with respect to shape at that region. The rapid rise of gust response when variation of design variables leads to low damping in any mode of motion is well known, and methods of constructing robust approximations for this case have been described before [11–13]. As shown in Fig. 9, as long as the speed of flight remains low, and hence, damping in all poles is not too close to zero (up to speeds of $V = 70 \sim 75$ m/ sec) one obtains good approximation match both for the deflection (Fig. 9a) and even for its derivative (local angle of attack).

IV. Conclusion

Analytical sensitivities with respect to configuration shape design variables have been derived for state-space models of aeroservoelastic systems excited by gust inputs. Minimum-state rational function approximations were used to transform aerodynamic load expressions from the frequency domain to the time domain, and sensitivities of such approximations were extended from terms associated with structural motions to terms associated with the downwash due to gusts. Sensitivity-based approximations of the resulting gust response behavior, including Taylor-series based direct approximations of the rms of the response, or Lyapunov equation solutions using Taylor-series based approximate system matrices were studied and compared. It was found that better approximate solutions for gust response can be obtained if approximate system matrices, based on Taylor series expansions, are used with repeated full Lyapunov equation solutions, compared with Taylor series approximations constructed directly for the gust response behavior functions of interest. Analytic sensitivities with respect to shape were shown to be accurate and reliable. Additional contributions of the work reported here include development of the most general state-space model with gust excitation where gust influence is separated from the structural influence in the system. Additionally, gust inputs are divided into gust zones to be transferred from the frequency to the time domain partly together and the rest separately. The analytical sensitivities with respect to shape variations include sensitivities of the motion of these gust zones when the shape varies. Good approximation accuracy in the presented cases was demonstrated even when a shape DV is changed as much as 100%. Overall, the paper contributes to the development of design-oriented analysis techniques for multidisciplinary design optimization of flight vehicles.

Appendix A: Gust Zones and Regions

For clarity, the classical linear aeroelastic equation including gust excitation formulated in the Laplace domain is

$$(s^2[M] + s[C] + [K] - q_D[Q(s)])\{\xi(s)\} = \frac{q_D}{V}\{Q_G(s)\}w_G(s) \tag{A1}$$

Here $\{Q_G(s)\}$ is actually a Laplace-transformed aerodynamic force coefficients vector. The induced angle of attack at some station x is defined as follows

$$\alpha(s) = \frac{w_G^{\mathrm{ref}}(s)}{V} e^{-s[(x-x_{\mathrm{ref}})/V]} \tag{A2}$$

where the gust profile w_G^{ref} is measured at some reference point (see Fig. 1). However, it makes it hardly realistic to generate good approximations for the gust vector using the formulation above [Eq. (A1)] especially in complex cases of the whole aircraft configuration. For the aircraft, the distance $x - x^{\mathrm{ref}}$ becomes large enough to exhibit a highly spiral shape at high frequencies as presented in [5]. This spiral curves cannot be correctly approximated by a rational polynomial expression. Therefore, the gust force is divided into a few gust zones, each with different reference point. This complicates the problem by introducing additional states into the state-space model, however, it prevents generation of the spiral behavior by keeping each distance $x - x_{\mathrm{ref}}$ relatively small. As mentioned above in this formulation the vector $\{Q_G(s)\}_{n\times 1}$ becomes an aerodynamic force coefficient matrix $[Q_G(s)]_{n\times n_G}$. This matrix is then approximated by rational functions. In this work we go step forward by developing the equations for the more general case where the matrix $[Q_G(s)]_{n\times n_G}$ is further divided into two regions. The first region $[Q_G(s)]_{n\times m}$ [see Eq. (8)], is approximated all together, whereas the rest of the columns of the gust aerodynamic force coefficient matrix are approximated each by its own rational function. These columns usually have different behavior patterns from the rest of matrix (which is related to the first region), and therefore approximated separately to better capture the behavior.

The choice of the gust zones, as well, which gust column to relate to which region, depends on the problem solved. Usually for a whole aircraft configuration it is wise to divide the wing into one or two zones. An additional gust zone is created for the tail. In the case of a very wide wing, or for the high sweep angle wing, the distance $x - x_{\mathrm{ref}}$ might become large enough to make it hard to obtain an adequate approximation. In this case extra zones are added. The gust columns are then plotted in the Re–Im plane for the different k values and the user might decide on the sequence for the two regions. In some cases the division into regions is not necessary and the whole matrix $[Q_G(s)]_{n\times n_G}$ is approximated by one function. This is a particular case of the general formulation presented in this article.

Appendix B: The Rational Approximation of the Delay Transfer Function

The general rational approximated (polynomial ratio) filter of the order n_e for $e^{-T_i s}$ can be presented as follows:

$$e^{-T_i s} \approx \frac{a_{n_e-1}(T_i s)^{n_e-1} + a_{n_e-2}(T_i s)^{n_e-2} + \ldots + a_1(T_i s) + a_0}{(T_i s)^{n_e} + b_{n_e-1}(T_i s)^{n_e-1} + \ldots + b_1(T_i s) + b_0} \tag{B1}$$

Expanding an exponent into Taylor series Eq. (B1) becomes

$$\begin{aligned}
&[(T_i s)^{n_e} + b_{n_e-1}(T_i s)^{n_e-1} + \ldots + b_1(T_i s) \\
&\quad + b_0]\left\{\sum_{j=1}^{2n_e-1}\frac{(-1)^j}{j!}(T_i s)^j + O[(T_i s)^{2n_e}]\right\} \\
&\quad \approx a_{n_e-1}(T_i s)^{n_e-1} + a_{n_e-2}(T_i s)^{n_e-2} + \ldots \\
&\quad + a_1(T_i s) + a_0
\end{aligned} \tag{B2}$$

where $O[(T_i s)^{2n_e}]$ is a truncation error of the order $2n_e$. Finally, the comparison of the coefficients in the expression above gives the system of equations, which can be divided into two subsystems solved separately: the first subsystem

$$\left\{\sum_{j=0}^{n_e-1}\frac{(-1)^j}{(i+j+1)!}b_{n_e-j-1} = \frac{1}{i!}, \quad i = 0, 1, \ldots, n_e - 1\right. \tag{B3}$$

provides the solution for $b_0, b_1, \ldots, b_{n_e-1}$, whereas the rest coefficients $a_0, a_1, \ldots, a_{n_e-1}$ are obtained as follows:

$$a_i = \sum_{j=0}^{i} \frac{(-1)^{i-j}}{(i-j)!} b_j, \qquad i = 0, 1, \ldots, n_e - 1 \tag{B4}$$

As an example, for the third order filter ($n_e = 3$), Eq. (B3) becomes

$$\begin{cases} b_2 - \frac{1}{2} b_1 + \frac{1}{6} b_0 = 1 \\ \frac{1}{2} b_2 - \frac{1}{6} b_1 + \frac{1}{24} b_0 = 1 \\ \frac{1}{6} b_2 - \frac{1}{24} b_1 + \frac{1}{120} b_0 = \frac{1}{2} \end{cases} \tag{B5}$$

whose solution is

$$\begin{bmatrix} b_2 & b_1 & b_0 \end{bmatrix} = \begin{bmatrix} 9 & 36 & 60 \end{bmatrix} \tag{B6}$$

and then using Eq. (B4) the rest coefficients are

$$\begin{gathered} a_0 = b_0 = 60, \qquad a_1 = -b_0 + b_1 = -24 \\ a_2 = \frac{1}{2} b_0 - b_1 + b_2 = 3 \end{gathered} \tag{B7}$$

Acknowledgment

Support for this research from NASA (Peter Coen, Grant monitor) is gratefully acknowledged.

References

[1] Karpel, M., and Strul, E., "Minimum-State Unsteady Aerodynamic Approximations with Flexible Constraints," *Journal of Aircraft*, Vol. 33, No. 6, 1996, pp. 1190–1196.

[2] Livne, E., "Integrated Aeroservoelastic Optimization: Status and Progress," *Journal of Aircraft*, Vol. 36, No. 1, Jan.–Feb. 1999, pp. 122–145.

[3] Mor, M., and Livne, E., "Minimum State Unsteady Aerodynamics for Aeroservoelastic Configuration Shape Optimization of Flight Vehicles," *AIAA Journal*, Vol. 43, No. 11, Nov. 2005, pp. 2299–2308.

[4] Giesing, J. P., Rodden, W. P., and Stahl, B., "Sears Function and Lifting Surface Theory for Harmonic Gust Fields," *Journal of Aircraft*, Vol. 7, No. 3, 1970, pp. 252–255.

[5] Karpel, M., Moulin, B., and Chen, P. C., "Dynamic Response of Aeroservoelastic Systems to Gust Excitation," *The CEAS/NVL/AIAA International Forum on Aeroelasticity and Structural Dynamics*, 2003.

[6] Rodden, W. P., and Johnson, E. H., *MSC/NASTRAN Aeroelastic Analysis User's Guide*, MacNeal-Schwendler Corporation, 1994.

[7] Bryson, A. E., and Ho, Y. C., *Applied Optimal Control*, Ginn and Company, Waltham, MA, 1969, p. 334.

[8] Schaeffer, H. G., *MSC.NASTRAN Primer for Linear Analysis*, 2nd ed., MSC Software, Santa Ana, CA, 2001.

[9] Yurkovich, R., "Status of Unsteady Aerodynamic Prediction for Flutter of High Performance Aircraft," *Journal of Aircraft*, Vol. 40, No. 5, Sept.–Oct. 2003, pp. 832–842.

[10] Chen, P. C., Liu, D. D., and Livne, E., "Unsteady Aerodynamic Shape Sensitivities for Airplane Aeroservoelastic Configuration Optimization," *Journal of Aircraft*, Vol. 43, No. 2, 2006, pp. 471–481.

[11] Livne, E., "Alternative Approximations for Integrated Control/Structure Aeroservoelastic Synthesis," *AIAA Journal*, Vol. 31, No. 6, June 1993, pp. 1100–1108.

[12] Engelsen, F., and Livne, E., "Quadratic Stress Failure Constraints for Structures Under Combined Steady and Random Excitation," *AIAA Journal*, Vol. 42, No. 1, Jan. 2004, pp. 132–140.

[13] Engelsen, F., and Livne, E., "A Design-Oriented Mode Acceleration Method for Lyapunov's Equation Based Random Gust Stresses in Aeroservoelastic Optimization," *Journal of Aircraft*, Vol. 41, No. 2, March–April 2004, pp. 335–347.